Proc. of SPIE Vol. 0748, Structural Mechanics of Optical Systems II, ed. A.E. Hatheway (Jan 1987) Copyright SPIE

Mirror Deformations Due to Thermal Expansion of Inserts Bonded to Glass

Bijan Iraninejad, Jacob Lubliner, Terry Mast, and Jerry Nelson

Department of Civil Engineering, Space Sciences Laboratory,
Astronomy Department, and Lawrence Berkeley Laboratory,
University of California, Berkeley, California 94720

Abstract

The support of mirrors often requires bonding inserts into holes in the mirror material. Temperature change and shrinkage of the bonding material and temperature change of the insert produce stresses that deform the optical surface Using both classical analytical methods and finite element techniques the deformation of plates and shells due to temperature and shrinkage effects are computed. The depth of the hole can be chosen to minimize the deflection of the optical surface. A variety of geometries which include hole diameters both large and small compared to the plate thickness are studied. In addition to the general formulation of the problem, some quantitative results for the Keck Observatory Ten Meter Telescope mirror segments are presented.

Contents

1 Introduction
2. Large Hole
  2.1 Effect of Bending Moment
  2.2 Effect of Radial Force
    2.2.1 Neutral Plane
    2.2.2 Deflection of Plates
    2.2.3 Deflection of Shells
    2.2.4 Neutral Plane Shift in Shells
  2.3 Hexagonal Versus Circular Mirrors
  2 4 Finite Element Calculations
  2.5 Radial Support Design and Performance
3 Small Holes
  3.1 Effect of Bending Moment
  3.2 Effect of Radial Force
  3 3 Insert Bonded in a Central Hole
    3.3.1 Neutral Plane
    3.3.2 Optimum Glue Thickness
  3.4 Multiple Holes

1. Introduction

The primary mirror of the Keck Ten Meter Telescope, currently under construction and scheduled for completion in 1990, consists of 36 hexagonal segments The design of the telescope and the segment support systems have been described in previous S P I E Proceedings and an extensive series of Keck Observatory internal reports and technical notes.

The support system for each segment consists of two kinematically decoupled sub-systems: an axial support system which carries the axial component of gravity (forces normal to the segment surface) and a radial support system which carries the transverse or radial component of gravity. Both the axial and radial support systems require attaching the metallic support structures to the glass-ceramic mirror segments The attachment is made by bonding the metallic support components into holes in the convex side of the mirror. Thermal expansion of the bonding material and support components will cause deformation of the segment and thus degradation of the image quality. This study addresses the deformation of mirrors due to thermal expansion of inserts bonded into holes

Each hexagonal segment is a uniform thickness meniscus with a radius of curvature of 35m The segment is 0.9 meters on a side and 0 075 meters thick The segment material is low thermal expansion glass-ceramic Zerodur (see Section 2 5 for material properties)

The diameter of the central blind hole, which houses the radial support system, is 0.254 meters or more than three times the mirror thickness. The holes needed for the axial support system are 0.018 meters in diameter or about one quarter the mirror thickness. In developing closed form expressions for the deformations we make assumptions which depend on the relative size of the hole. Thus the study is divided into two parts, addressing large and small diameter holes separately.

Our analytic studies are made for a circular segment with an area equal to that of the actual hexagonal segments. Finite element calculations are used to study the hexagonal segments.

2. Large Hole

For the Keck telescope segments the radial or in-plane component of gravity is carried by a radial support system of a thin flexible diaphragm and a rigid post. These are shown schematically in Figure 1. The outer radius of the thin diaphragm is attached to the mirror and the central region of the diaphragm is bolted to a support post The design calls for a stainless steel diaphragm with thickness of 0.25 mm (10 mils) and Invar components to attach the diaphragm to the glass The assembly is bonded into a blind hole with a 0 254 m diameter To avoid coupling between the support systems, the segment center of gravity is in the plane of the diaphragm and the diaphragm plane is coplanar with the segment

Motivated by the above design we consider a plate with a central hole with a diameter larger than the plate thickness The radial support mechanism is not explicitly modeled, but its effect on the mirror is incorporated into the analysis by considering the forces and moments that the radial support applies to the glass. Thermal expansion and curing of the adhesive will exert axisymmetric stresses on the edge of the hole. The effect of these stresses depends on their depth in the hole and can be decomposed into the effect of a ring moment about the edge of the hole and that of a radial ring force at a suitable depth in the hole

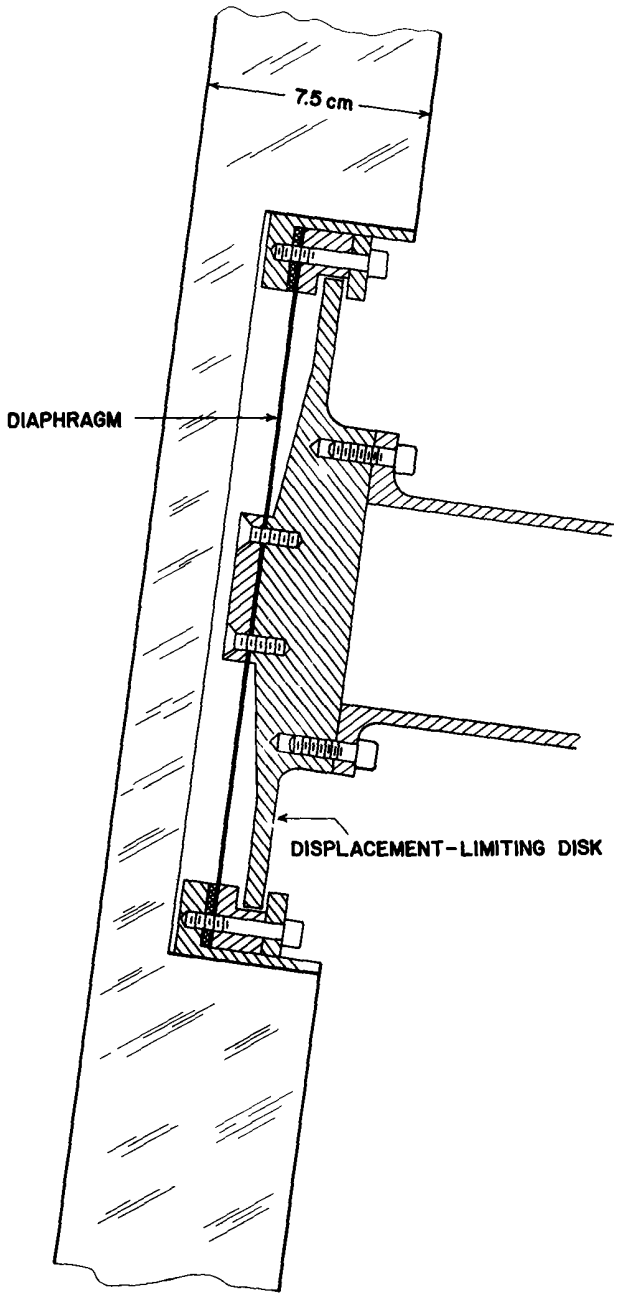

Figure 1 Radial Support Assembly, Original Design.

2.1 Effect of Bending Moments

The plate deflections caused by an axisymmetric line moment, M, applied around the circumference of a blind hole of radius b at the center of a circular plate with radius a is formulated. Figure 2 shows the geometry Let the depth of the hole be $(1-\beta)h$ and the thickness of the remaining plug be βh.

The deflection is obtained by considering two elementary cases:

1) bending of a circular plate of radius b and thickness βh with an unrestrained edge and subjected to bending moment and radial in-plane force around the edge, and

2) bending of an annular plate with thickness h, inner radius b, outer radius a with an unrestrained inner edge and subjected to bending moment and radial force around the inner edge.

Satisfying the equilibrium and continuity requirements at radius b for these cases results in the following expressions for the deflection

For $r \leq b$

$$z(r) = \frac{-K_1 M b^2}{2D'(1+\nu)}[1-(r/a)^2] \tag{1 1}$$

For $r \geq b$

$$z(r) = \frac{-K_2 M b^2}{D[1-(b/a)^2]}\left[\frac{(r/a)^2}{2(1+\nu)} + \frac{\ln(r/a)}{1-\nu} + z_0\right] \tag{1 2}$$

where

$$z_0 = -\frac{(b/a)^2}{2(1+\nu)} - \frac{\ln(b/a)}{(1-\nu)} \tag{1 3}$$

$$K_1 = -\frac{\Phi_0\Phi_1/\beta^3}{1+\Phi_0} \tag{1 4}$$

$$K_2 = \frac{\Phi_1}{1+\Phi_0} \tag{1.5}$$

$$\Phi_0 = \frac{1/\gamma + (b/a)^2}{1-(b/a)^2}\beta^3 \tag{1.6}$$

$$\Phi_1 = \frac{(\gamma+\beta)(1+\beta^3/\gamma)}{\Phi_2} \tag{1.7}$$

$$\Phi_2 = \gamma + 4\beta - 6\beta^2 + 4\beta^3 + \beta^4/\gamma \tag{1.8}$$

$$D = Eh^3/12(1-\nu^2) \tag{1 9}$$

$$D' = E\beta^3 h^3/12(1-\nu^2) \tag{1.10}$$

$$\gamma = \frac{1-\nu}{1+\nu} \tag{1 11}$$

The plate material is isotropic and linearly elastic, ν is the Poisson's ratio, E is the modulus of elasticity, and M is the moment intensity and has units of $force \times length / length$.

The shape of the deformations comes from two terms; one that varies as r^2 and one that varies as $\ln r$. The depth of the central hole only effects the magnitude of deformations through K_1 and K_2 terms; the variation of these terms as a function of β and for several values of b/a is shown in Figure 3 If $\beta h/b$ is very small, the deformation of the central region $(r < b)$ is governed by the membrane action and the above formulation does not apply.

In the limiting case for a through hole, $(\beta = 0.0)$, K_2 is equal to unity and the slope of the surface is given by

$$\frac{dz(r)}{dr} = \frac{-Mb^2}{D[1-(b/a)^2]}\left[\frac{r/a^2}{(1+\nu)} + \frac{1}{r(1-\nu)}\right] \tag{2}$$

The resulting image degradation can be characterized by the diameter of the image that contains a given fraction of the energy from a point source. The maximum slope occurs at the edge of the hole and results in a 100% enclosed energy image diameter of

$$\theta(100) = \frac{4Mb^2}{D[1-(b/a)^2]}\left[\frac{b/a^2}{(1+\nu)} + \frac{1}{b(1-\nu)}\right\} \tag{3}$$

Since the slope monotonically increases towards the center one can readily find the image size for other enclosed energy fractions. For a fraction f of the energy, the light comes from an annulus with an inner radius of

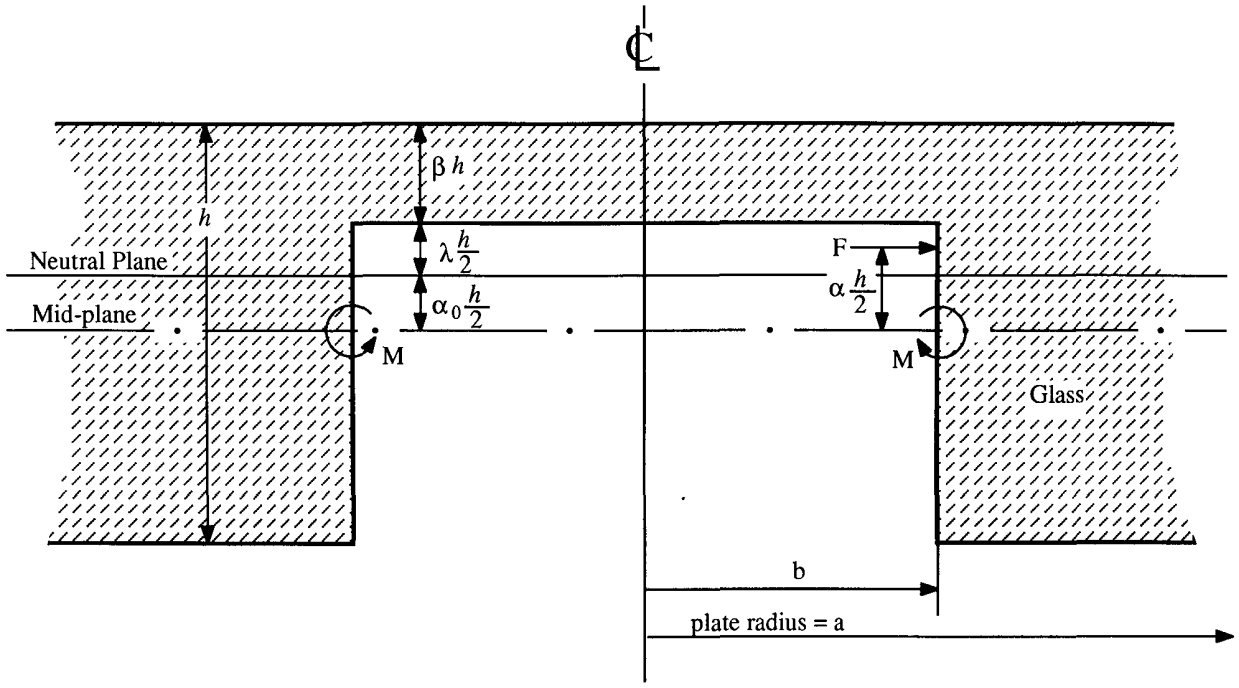

Figure 2. Central Hole Geometry

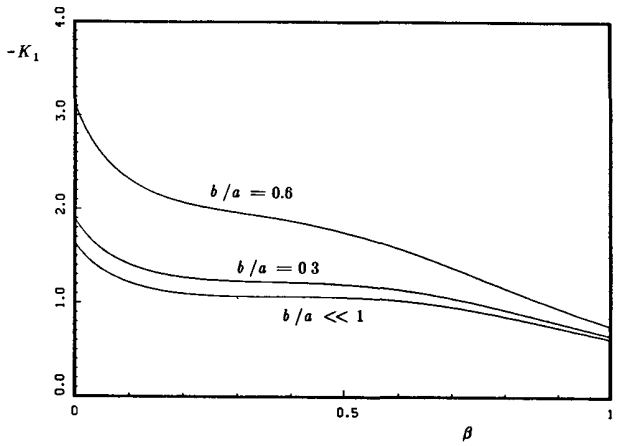

Figure 3 a Variation of K_1, vs β.

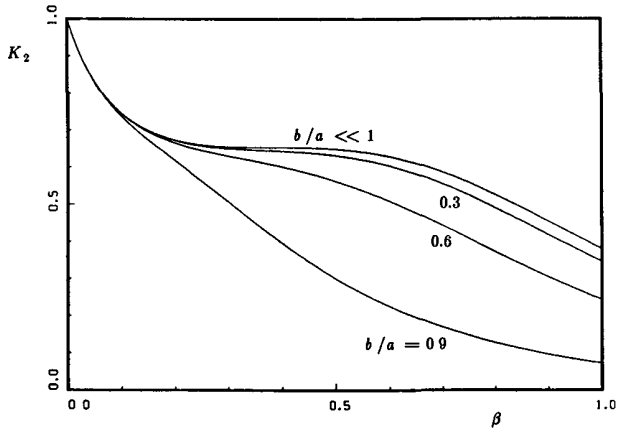

Figure 3 b Variation of K_2 vs β.

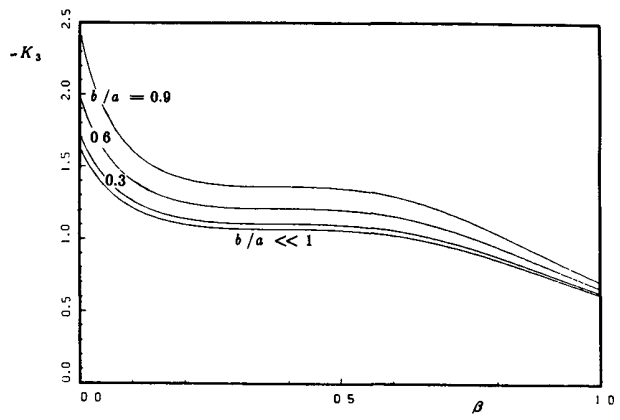

Figure 3.c Variation of K_3 vs β

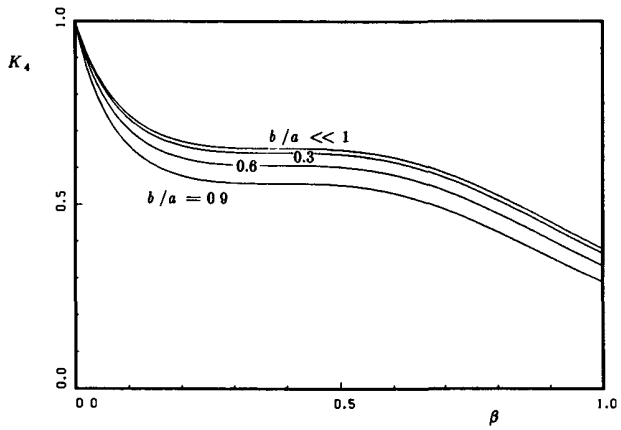

Figure 3.d Variation of K_4 vs β

$r_f = ((1-f)a^2 + fb^2)^{1/2}$. For $r_f << a$, the image diameter containing the fraction f of the energy is approximately given by

$$\theta(f) \doteq \theta(100)\frac{b}{r_f} \tag{4}$$

Note from Equation 1 2 that for $b/a << 1$, the amplitude of the deformations varies as the square of the hole radius b and terms defined in Equations 1 4 through 1 7 become independent of both the plate and hole radii For this case, the constants z_0, K_1 and K_2 can be written in simplified form as

$$z_0 = -\frac{\ln(b/a)}{(1-\nu)} \tag{5 1}$$

$$K_1 = -\frac{\gamma+\beta}{\gamma\Phi_2} \tag{5 2}$$

$$K_2 = \frac{\gamma+\beta}{\Phi_2} \tag{5.3}$$

The variation of K_1 and K_2 for the above case is also shown in Figure 3.

The deformation of shells due to moment loading in the central blind hole is not analyzed, but it is expected that, to first order, the resulting deformations will be the same as that of the plate

2.2 Effect of Radial Force

Assume the axisymmetric radial force F in the hole is applied at a distance above the midplane of $\alpha h/2$. The units of F, the force density, is *force/length* and α is dimensionless.

2.2.1 Neutral Plane

For a flat plate with a through hole, an axisymmetric radial force applied at the midplane will not cause any bending deformation. But by making the hole a blind hole (β>0.0), the symmetry is destroyed and the plate bends The plate bends up if $\alpha = -1$ and it bends down if $\alpha = 1$ It follows that there exists an intermediate location, $\alpha = \alpha_0$, which gives zero bending We call this the neutral plane and it is a distance $\alpha_0 h/2$ above the midplane. Requiring the bending moments to vanish everywhere inside the plate gives an expression for α_0 (Lubliner, Keck Observatory Technical Note No. 186)

$$\alpha_0 = \frac{\beta(1-\beta)}{\beta+\gamma} \tag{6}$$

The variation of α_0 as a function of β is plotted in Figure 4 Equation 6 is only applicable if $h < b$, and shows that α_0 does not depend on the radius of the hole. The neutral plane reaches its maximum distance from the midplane at $\beta = (\gamma^2+\gamma)^{1/2} - \gamma$. For $\nu = 0.24$, the smallest hole depth that results in a neutral plane outside the glass corresponds to $\beta = 0.381$.

Ideally, inserts should be located so that the forces caused by their expansion lie in the neutral plane, thus producing no bending. Since real inserts will have a finite depth, this means that generally the insert hole will have to be deeper than the neutral plane. If the distance from the bottom of the insert and the center of the insert line of force is $\lambda h/2$, then placing the line of force in the neutral plane requires a hole depth defined by

$$2\beta = [(2\gamma+\lambda)^2 + 4\gamma(1-\lambda)]^{1/2} - 2\gamma - \lambda \tag{7}$$

Equation 7 is plotted in Figure 5.

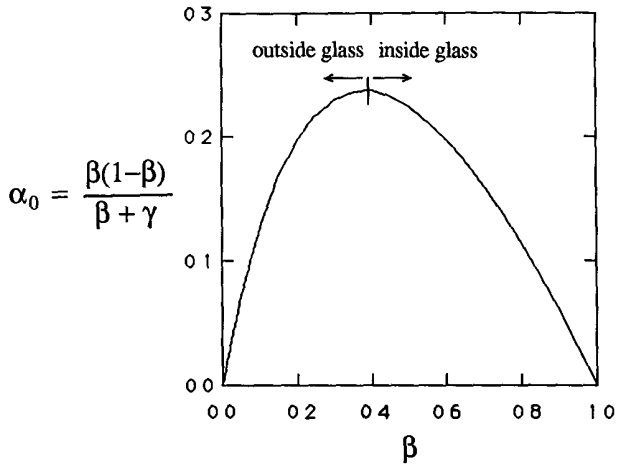

Figure 4 Neutral Plane Shift, α_o, vs β for Plates

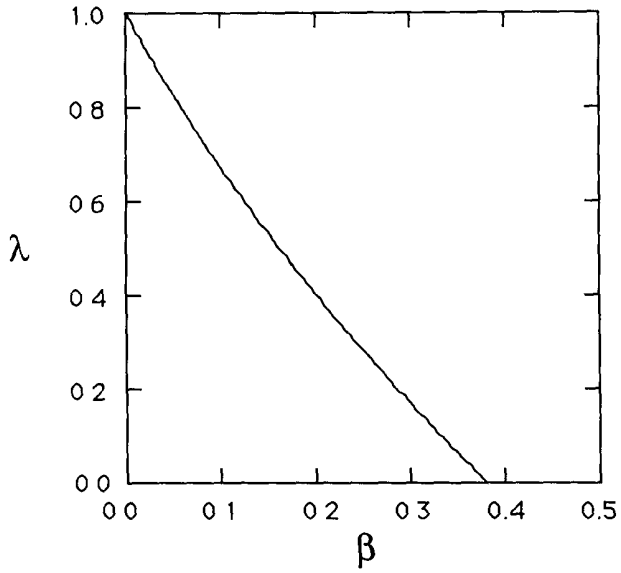

Figure 5. Neutral Plane Distance from the Bottom of Plug , λ, vs β for Plates.

2.2.2 Deflection of Plates

The surface deformations due to an axisymmetric radial force can be formulated using the same procedure discussed in Section 2 1. If F is the intensity of the axisymmetric ring loading, then the plate deflections are given by

$$z(r) = -\frac{K_3 m b^2}{2D'(1+\nu)}[1-(r/a)^2] \qquad (8\,1)$$

for $r \leq b$ and

$$z(r) = -\frac{K_4 m b^2}{D[1-(b/a)^2]}\left[\frac{(r/a)^2}{2(1+\nu)} + \frac{ln(r/a)}{1-\nu} + z_0\right] \qquad (8\,2)$$

for $r \geq b$, where

$$m = (\alpha - \alpha_0)\frac{h}{2}F \qquad (8\,3)$$

$$K_3 = -\frac{\gamma+\beta}{\gamma\Phi_4} \qquad (8\,4)$$

$$K_4 = \frac{\gamma+\beta}{\Phi_3\Phi_4} \qquad (8.5)$$

$$\Phi_3 = 1 + \gamma(b/a)^2 \qquad (8\,6)$$

$$\Phi_4 = \frac{\gamma}{\Phi_3} + (3 + \frac{1}{\Phi_3})\beta - 6\beta^2 + 4\beta^3 + \beta^4/\gamma \qquad (8\,7)$$

Note that the deflections vanish if the force is applied at $\alpha = \alpha_0$. The depth of central hole effects the amplitude of deformations through K_3 and K_4. Figure 3 shows the variation of K_3 and K_4 as a function of β.

If $b/a \ll 1$, then Φ_3 becomes unity, Φ_4 becomes equal to Φ_2, $K_1 = K_3$, $K_2 = K_4$, and with $M = m$, Equations 8 1 and 8 2 become equal to Equations 1.1 and 1 2.

2.2.3 Deflection of Shells

If the plate has an initial curvature, approximately spherical with a radius of curvature R such that $R \gg a$, then it is governed by the theory of shallow shells (Timoshenko and Woinowsky-Krieger, p.558). A perturbation approach is used to obtain a first order approximation to the shell deflections. The peak deformation is written as $\Delta_0 + \Delta_1$ In principle, $\Delta_0 = z(0) - z(a)$, is the peak plate deformation (Equations 8.1-8 7) and Δ_1 is the additional deformation due to the shell effect. If $b/a \ll 1$, then

$$\Delta_1 = \frac{2(F-X)a^2b^2}{RD(1-(b/a)^2)}K_5 \qquad (9.1)$$

where for $b/a \ll 1$,

$$X = \frac{F\beta}{\gamma\Phi_2}[\gamma\Phi_2 + 3\gamma(1-\beta)\alpha_1], \qquad (9\,2)$$

R is the radius of curvature of the segment or shell, and α_1 is defined below. The shell effects for radii less than b is small and is not considered in computing Δ_1. The quantity K_5 is given by Roark and Young, Case 2k, page 342 To first order

$$K_5 = \frac{1}{64}\left(\frac{7+3\nu}{1+\nu}\right) \qquad (10)$$

Roark's complete solution can be used for numerical calculation of K_5 including all orders For $b = 0\,127$ and $\nu = 0\,24$ the first order value of $K_5 = 0\,0973$. Calculating to all orders gives $K_5 = 0.116$

2.2.4 Neutral Plane Shift in Shells

For plates, the neutral plane was defined as the plane within which forces will cause no bending For shells, there is no plane that causes zero deflection However, we can define an approximate neutral plane as that position where the maximum plate deflection is canceled by the deflection due to the shell effects Let $\alpha_{shell} = \alpha_0 + \alpha_1$ where α_{shell} is the neutral plane location for a shell and α_0 is the previously calculated neutral plane location for the plate problem The approximate shift in the neutral plane, α_1, caused by the shell effects is obtained by setting $\Delta_0 + \Delta_1 = 0$, and solving for α_1. The results are approximate because we ignore the deformation over the zone with radii less then b and let $\Delta_0 = z(0) - z(a) \approx z(b) - z(a) \approx -z(a)$. We then find

$$\alpha_1\frac{hR}{a^2} \doteq \frac{4\gamma\Phi_2K_5}{(\beta+\gamma)^2}\left\{\frac{1-(b/a)^2}{2(1+\nu)} - \frac{1}{1-\nu}ln(b/a)\right\}^{-1} \qquad (11)$$

Note that unlike α_0, α_1 is a function of the ratio b/a. Figure 6 shows the variation of α_1 as a function of β for a range of b/a ratios. The range of b/a values is selected to cover the range in which Equation 11 is applicable.

As an example consider the case of a through hole ($\beta = 0.0$, and $\alpha_0 = 0\,0$) in Zerodur. For typical Keck Observatory parameters, $a = 0.818$m, $b = 0.127$m, $h = 0\,075$m, and $R = 35\,0$m, Equation 11 gives a neutral plane shift of 1 56 mm. A finite element calculation of this shift gives 1.6mm (Iraninejad, Keck Observatory Technical Note No. 190) in excellent agreement with the analytic result.

For the Keck Observatory segments, the radial support hole is a blind hole with the remaining plug thickness of 0.02m ($\beta = 0.267$). This gives $\alpha_0(h/2) = 8.34$ mm and $\alpha_1(h/2) = 1.65$ mm. Thus the neutral plane is located 9.99mm in front on the midplane.

2.3. Hexagonal Versus Circular Mirrors

The deflection of hexagonal mirrors for the Keck Observatory was estimated by calculating the results for an area equivalent circle ($a = 0.818$m). However, a hexagon with a side length of 0.9m will have a larger peak deflection than the circle of radius 0.9m since the material removed will reduce the stiffness. Thus, for the actual hexagons, we expect a peak deflection larger than the values obtained by using the closed form solutions for area equivalent circle

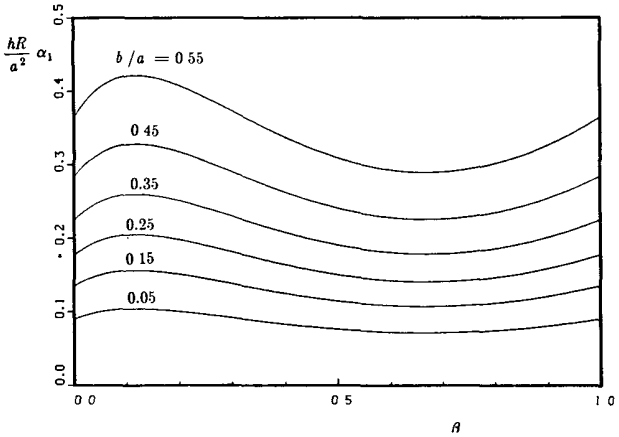

Figure 6. Contribution of the Shell Effects to Neutral Plane Shift, $Rh\,\alpha_1/a^2$, vs β

2.4 Finite Element Calculations

For a limited number of cases the deflections were calculated using the finite element program SUPERSAP (Iranine-jad, Keck Observatory Technical Note No 190) Table 1 below summarizes the comparison between the analytic and finite-element results. For all the cases the nominal values for the Keck Observatory mirror segments are used The thickness of the plug above the hole is assumed to be $\beta h = 0\,02$ m

Table 1. Peak-to-Peak Deflections
(Deflections in nanometers)

Configuration	Analytic circle	SUPERSAP circle	SUPERSAP hexagon
Moments ($M = 1\,0$N-m/m)			
Plate-through hole	13.9	13 0	15 0
Plate-blind hole	11 2	11 9	11 8
Shell-through hole	13 9	13.7	14.9
Forces applied at midplane ($F = 1.0$N/m)			
Plate-through hole	0 000	0.000	0.000
Plate-blind hole	0 094	0.071	0 100
Shell-through hole	0 022	0 022	0 024

We note there is generally good agreement between the analytic and finite element results

2.5. Radial Support Design and Performance

We now turn to an application of these general results and analyze the effects of specific radial support insert designs We first consider an "old design" that was found to be inadequate, and then an improved "new design" created to reduce the deformations found with the old design.

Old Design

Consider an Invar ring glued into a hole in a segment We begin by finding the pressure that the Invar ring exerts on the wall of the hole in the segment as the temperature changes. This problem is solved by considering the thermal interactions of three annuli, metal, glue, and glass (Nelson, Keck Observatory Technical Note No 184).

We assume the following material properties.

Invar Ring	
E	$2\,1\times10^{11}N/m^2$
ν	0 3
α_T	$2\times10^{-6}/^\circ C$
radial thickness	0.010 meters
Glue (Stycast)	
E	$7\,6\times10^{9}N/m^2$
ν	0 3
α_T	$25\times10^{-6}/^\circ C$
radial thickness	0.001 meters
Glass-ceramic	
E	$9\times10^{10}N/m^2$
ν	0.24
α_T	$5\times10^{-8}/^\circ C$
hole radius	0.127 meters
segment radius	0 818 meters

Because the glue layer is thin the resulting pressure is insensitive to the glue thickness.

In this design, the Invar (about 0 02m) and glass (0.075m) will be much wider (longer in axial length) than the glue (about 0 01m) so their effective stiffnesses will be larger than indicated by a naive application of formulas in Technical Note No 184. We will crudely estimate the increase in stiffnesses by doubling the assumed elastic modulus of the Invar and the glass. This roughly doubles the pressure and is mainly due to doubling the Invar E.

For the Keck Telescope we anticipate the Invar ring will be glued at $20^\circ C$ and the system must operate within specifications down to $-6^\circ C$. The glue shrinkage during curing will be 10^{-3} which is equivalent to $\Delta T = 40^\circ C$. Thus the combination of temperature change and shrinkage give an effective $\Delta T = 66^\circ C$. Using the formulae in Technical Note 184 gives a pressure of $P_2 = 4\,07\times10^{6}N/m^2$ or 589 psi.

Given this pressure we estimate the resulting deflections on the plate We assume the glue pressure line is not perfectly centered on the neutral plane, but is displaced a distance $\delta = 1$mm, a plausible installation error The induced moment is

$$M = 4.07\times10^{6}(0.01)(0.001) = 40\,7 \text{ N-m/m}$$

The plate bending and image blur are found from Equation 8 2 The peak deflection is 373nm and $\theta(100) = 1.14$ arc seconds.

The allowed image blur from thermal effects in the mount is about 0.02 arc seconds, thus this simple ring design is not acceptable.

New Design

Because of the unacceptable performance of the simple Invar ring, a new design was created which is azimuthally and radially stiff, but which has diametral compliance (Weitzmann, Keck Observatory Technical Note No. 165). The Invar ring is connected to six bonding pads through leaf springs (Figure 7). For a leaf spring thickness of 0.4 mm and a temperature change of $\Delta T = 26^\circ C$ the radial force on the glass is 25.6 N/m.

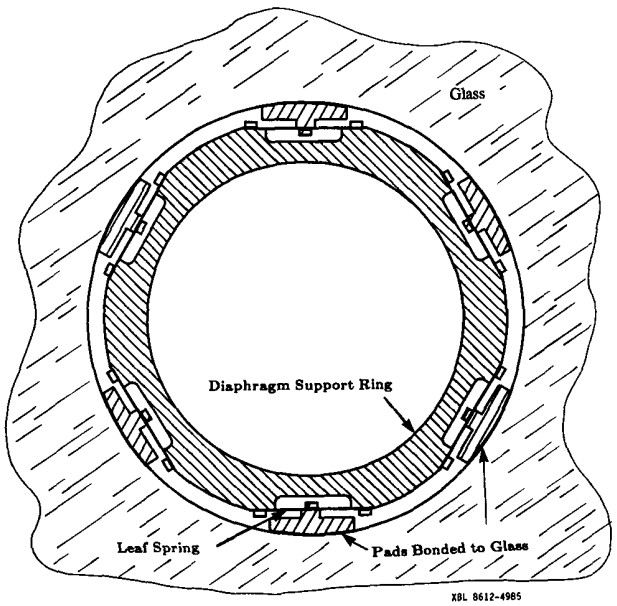

Figure 7. Radial Support Assembly, Final Design.

The location of the center of gravity of the segment is 39.7mm in front of the convex surface, i e 2 2 mm in front of the midplane. The diaphragm plane must be at the center of gravity A modification of new design places the center of the leaf springs at the same position as the diaphragm. Since the neutral plane is 9.99 mm from the midplane, there is a displacement of the thermal expansion forces of 7 8 mm from the neutral plane.

Using these values for the forces and displacement from the neutral plane we can calculate the moment $M = 0.2$N-m/m. Using the analytic results for a flat plate from Table 1, and Equation 1 2, we thus predict a peak deflection of 2 2 nm and $\theta(100) = 0\ 005$ arc seconds This easily meets the image quality error budget.

3. Small Holes

In the Keck Observatory segment design the axial component of gravity is carried by three whiffletrees Each whiffletree is attached to the glass at 12 locations. The location of the attachment points and the geometry of the whiffletree (pivot point locations) is optimized to result in a minimum rms deflection under gravity loading in the axial direction. Figure 8 is a schematic drawing of the axial support system The actuators are shown as circles and the 36 support points as solid dots The whiffletrees are designed to be statically determinate systems, therefore the axial motion of the actuators, required for active control of the segment positions, will not result in redistribution of forces and the optical surface maintains its shape At each axial support point a metal insert is bonded into a blind hole in the glass. A thin flexible rod connects the insert to the whiffletree The diameter of the hole is about a quarter of the thickness of the mirror, therefore, the previously developed formulation for the affects of inserts in large holes is not applicable to this case.

To develop an understanding for the effects of axisymmetric bending moments and radial forces in small holes the finite element method was used Both plates and shells were considered The hole depth was varied from no hole to a through hole. The axial position of the forces was varied from the top to the bottom surface Detailed results of this study are given in Keck Observatory Technical Note No 194 In the following two sections we summarize the results.

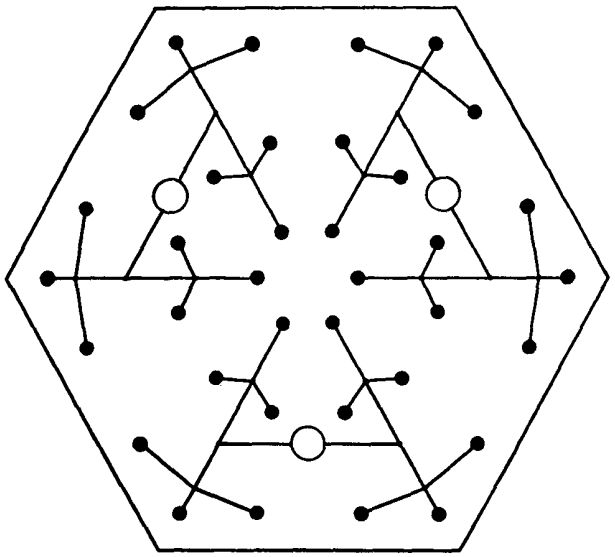

XBL 8212-11990

Figure 8. Axial Support Assembly

The shape of the top surface deflection for the through hole and the no hole configurations were compared with thin plate bending predictions (Equations 1 and 8) These comparisons showed that for radii beyond 10 cm the top surface deflections from the two calculations are in good quantitative agreement For radii near the hole the surfaces differ due to the local deformations We are primarily interested in the large area outside the hole Thus, we use for a one parameter characterization of the top surface the difference between the deflections at a radius of 10 cm and the edge deflection, Δ_{10}

3.1 Effect of Bending Moment

The deflections from moments applied at a radius b depend on whether the axial position, α, is within the empty region of the hole or the plug region of the hole For moments within each of these regions the deflection is independent of the axial position.

For moments applied to the edge of the hole the deflections far from the hole are essentially those predicted for large holes (Equation 1). When the moment is applied inside the glass plug, finite element analysis of the Keck Observatory segments with $b = 0.009$ m shows that the deformations are reduced to about 0.38 of those when the moment is applied to the hole. A simple analytical model for describing the above phenomenon was formulated (Iraninejad, Keck Observatory Technical Note No 194) which predicts a reduction factor of $\frac{1 + b^2/a^2}{1 + \gamma}$. This formulation suggests that for the Keck Observatory segments the surface deformations is reduced by a factor of 0 38, which exactly matches the numerically generated results.

3.2 Effect of Radial Force

The deflections due to an axisymmetric ring of forces at radius b were studied for various hole depths and axial position of forces for the Keck Observatory segments ($a = 0\ 818$m, $h = 0\ 075$ m, $b = 0\ 009$ m)

For each hole depth there is an axial position of force application where Δ_{10} is zero. This defines a neutral plane for each hole depth The neutral plane for small holes always remains close to the midplane. As the hole depth varies from no hole ($\beta = 1$) to a through hole ($\beta = 0$) the neutral plane varies from the midplane to 3 mm above the midplane and then back to the midplane. Although this result clearly depends on b, we have not systematically studied this dependence. For the shell the neutral plane is shifted toward the top surface by a small additional amount Figure 9 shows the variation of the normalized neutral plane location, α_0 and α_{shell}, as a function of the plug thickness, β, computed using the finite element results.

In general the deflections are proportional to the distance from the neutral plane We conclude that the plate bending due to forces applied inside a small blind hole is well described by an equivalent moment given by the force times the distance to a neutral plane which is close to the midplane For a ring of applied force within the plug of the blind hole there is a canceling of the forces that get transmitted to the outer plate and this reduces the effective moment to about 40% of that when the forces are applied in the empty region

of the hole, just as we found for the applied moments The previously discussed analytical model for predicting the reduction factor for moments also applies to forces and gives a reduction factor of 0 38.

If one assumes that the forces are applied exactly at the bottom of the hole, then the deflection Δ_{10} is zero when the hole depth is 1 3 mm above the midplane (2 5 mm for the shell)

3.3 Insert Bonded in a Central Hole

The insert design considered for the Keck Telescope is shown in Figure 10 From Section 3.1 it is known that the optimum position of the hole bottom will be near the midplane However, the forces on the glass are not the simple ring of force assumed in Section 3.1, but instead are applied over the surface of the bottom of the hole. In this section, the neutral plane location for the designed insert assembly is computed and the optimum glue thickness is found For all cases, a temperature change of $\Delta T = -20^{o}\ C$ and a glue shrinkage of 10^{-3} are imposed

3.3.1 Neutral Plane

To establish the neutral plane location, an explicit finite element model of the glue and insert is made. The insert material is Invar and the glue is 1mm thick The glue, Invar, and glass properties are given in section 2 5.

Two geometries, one with no metal insert and only a uniform layer of glue, and another with both glue and Invar insert are considered. The following Table lists the computed neutral plane locations

Shift of Neutral Plane above the Midplane
(millimeters)

	plate	shell
glue only	1.56	2.60
glue and insert	1.24	2 76

Note that these results are similar to those found for a force applied at the bottom of a hole (See Section 3 2).

3.3.2 Optimum Glue Thickness

We consider three different cases and study the effect of change in the glue thickness on deformations measured by Δ_{10}. For all cases the bottom of hole is at the midplane, the Invar insert is 0.018 m in diameter and 0 01 m in height, the modeling is done such that the Invar insert and the glass do not interface each other, and the shell effects are ignored The results are summarized in Figure 11 First, in case I, consider a geometry with no metal insert and only a uniform layer of glue As shown in Figure 11, for glue thicknesses less than about 1mm the deflection caused by glue is proportional to the thickness.

We next consider the full model of glue and insert. The results are shown in curves II and III of Figure 11. Curve III gives the deflection when the coefficient of thermal expansion for the Invar is set to zero, therefore the insert acts as a constraint on the glue and limits the amount of force transferred to the glass. The deflection increases with glue thickness but levels off rapidly.

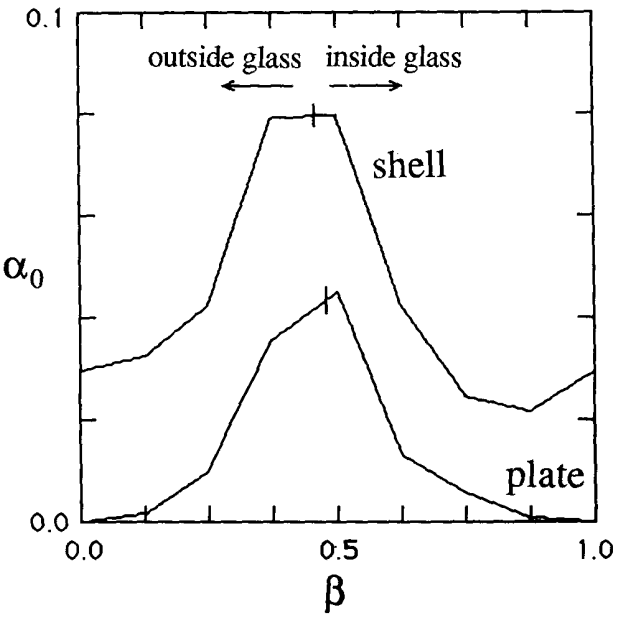

Figure 9 Neutral Plane Shift for Small Holes

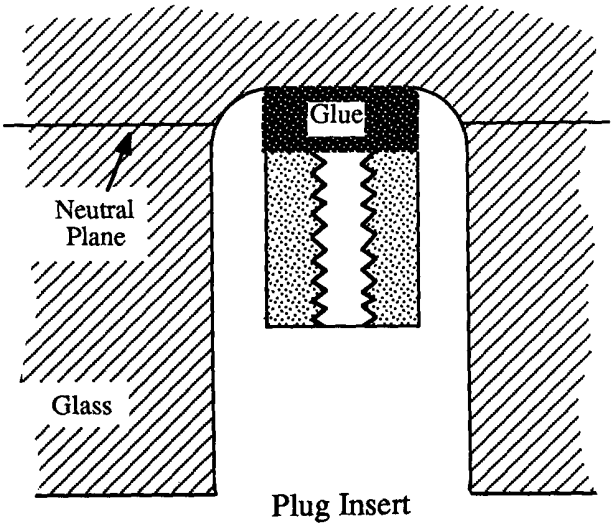

Figure 10. Hole/Insert Geometry.

Curve II shows the deformations when the coefficient of thermal expansion for the Invar is set to its realistic value given in section 2.5. At zero glue thickness, the expansion of Invar is directly responsible for bending the mirror Since the glue is substantially more flexible than the Invar, placing a layer of glue between the Invar and the glass will act as a buffer between the high expansion Invar and the low expansion glass This effect will reduce the forces transferred to glass and results in lower deflections. However, as the glue thickness increases above a certain level, the temperature/shrinkage effects in the glue begin to dominate and results in increasing deformations. Therefore, there exists an optimum glue thickness which is given by curve II. For the parameters assumed here the optimum glue thickness is 0.25 millimeters which results in $\Delta_{10} =$ 0.3 nm. The dependence of the above results on b and the modulus of elasticity of the materials was not studied.

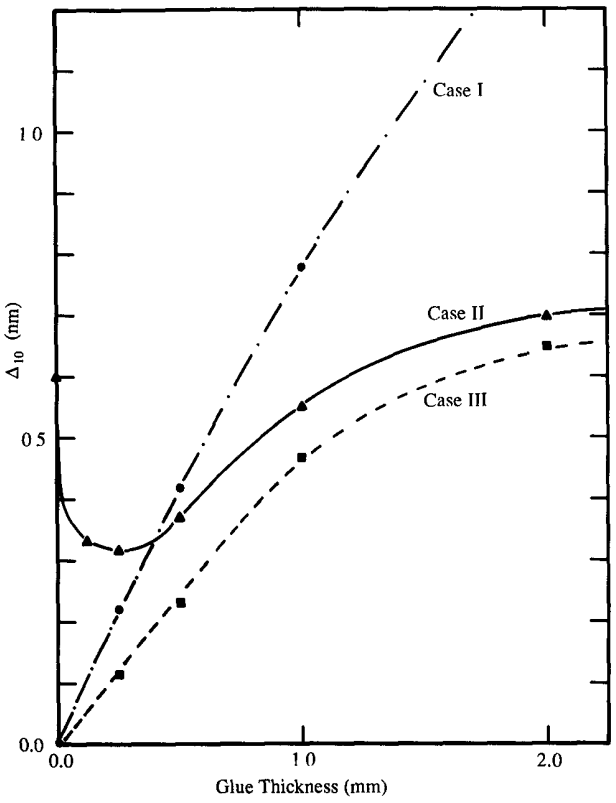

Figure 11. Δ_{10} Deflections vs Glue Thickness

3.4 Multiple Holes

For the Keck Observatory, there are 36 small holes for the whiffletree attachment. Thermal effects of the inserts will act coherently on all holes, so the net image blur from 36 inserts will be substantially more than from a single insert

We have only analyzed the axisymmetric case and have no predictions for deformations due to non-central holes. Even if we assume all inserts have the same deformation shape as that of a central hole, adding them together is difficult because there are both quadratic and logarithmic terms. The quadratic terms add linearly, but the logarithmic terms are relatively local and thus do not add in the same way.

Alternately, we can attempt to estimate the image blur from examining slopes instead of deflections. Again, a general solution is not available. As a practical matter, if one is willing to exclude the small area surrounding each insert that has large slopes, then the maximum slopes appear at the edge of the segment when a large number of inserts are used. This can be approximated by evaluating Equation 2 at $r = a$ and multiplying by the number of inserts. Thus

$$\theta_{\max} \doteq 4N_{inserts} \frac{dz(a)}{dr} \qquad (12)$$

References

Iraninejad, Bijan , Keck Observatory Technical Note No. 158, "Effect of Central Hole on Surface Deformations Under Uniform Radial Loading", May 1986.

Iraninejad, Bijan , Keck Observatory Technical Note No. 190, " Finite Element Study of Deformations Caused by the Central Hole Insert ", June 1986

Iraninejad, Bijan , Keck Observatory Technical Note No 194, " Surface Deformations Caused by Inserts ", December 1986

Lubliner, Jacob , Keck Observatory Technical Note No 185, "The Effect of Glue Shear on the Thermal Deformation of Laminated Circular Plates ", May 1986

Lubliner, Jacob , Keck Observatory Technical Note No. 186, "The Effect of a Radial Ring Force in a Blind Hole in a Large Plate", May 1986

Nelson, Jerry, and Terry Mast, Keck Observatory Technical Note No. 174, "Deformations Caused by Segment Inserts", June 1986

Nelson, Jerry , Keck Observatory Technical Note No. 181, "The Effect of Grinding Stresses in Bored Holes", May 1986.

Nelson, Jerry , Keck Observatory Technical Note No. 184, "Thermal Expansion of Three Concentric Annuli", May 1986.

Roark and Young, "Formulas for Stress and Strain", Fifth Edition, McGraw-Hill ,1975.

Timoshenko and Woinowsky-Krieger, "Theory of Plates and Shells", 2nd Edition, McGraw-Hill, 1959.

Weitzmann, Robert , Keck Observatory Technical Note No 165, "A Revised Radial Support Concept For TMT Segments", December 1985